Morphometry of Great Basin pluvial shore landforms: Implications for paleolake basins on Mars

Rossman P. Irwin III[1,2] and James R. Zimbelman[1]

Received 6 January 2012; revised 16 April 2012; accepted 25 May 2012; published 18 July 2012.

[1] Many basins with relict contributing valley networks and outlet valleys in the Martian highlands indicate past flowing and ponded water on the surface. These likely paleolakes motivate an investigation of pluvial shore landforms in the Great Basin region of the western United States, as confident identification of strandlines on Mars would facilitate analyses of its past hydrology and climate. The purpose of this study is to characterize the scale of Late Pleistocene erosional and depositional shore landforms in an endorheic setting, determine the preservation potential of similar forms from multiple epochs in early Martian history, and identify the data products that would be necessary to detect them. We use Differential Global Positioning System field surveys to measure the dimensions and elevations of shore landforms; compare shore platform widths to theoretical maxima; and note the minimum scale of landforms that have survived since the Late Noachian and Early Hesperian Epochs on Mars. We find that due to impact gardening and aeolian erosion, Martian highland paleolakes like those in the pluvial Great Basin would likely not have well-preserved shore landforms, unless they were unusually large and formed in the Late Hesperian or later. Individual strandlines are often not equally well expressed around an entire basin, so correlating shore landforms in plan view imaging and using their consistency in elevation as a hypothesis test for paleolakes can be challenging. Detection of younger shore landforms like those examined here would require meter-resolution imaging and topography such as stereo digital elevation models.

Citation: Irwin, R. P., III, and J. R. Zimbelman (2012), Morphometry of Great Basin pluvial shore landforms: Implications for paleolake basins on Mars, *J. Geophys. Res.*, *117*, E07004, doi:10.1029/2012JE004046.

1. Introduction

[2] Orbital imaging and topographic data have shown that the highland landscape of Mars is heavily cratered and dissected by branching valley networks [e.g., *Masursky et al.*, 1977; *Pieri*, 1980; *Hynek et al.*, 2010]. This multibasin landscape may have been favorable for ponding, depending on the ratio of water supply to evaporation loss [*Matsubara et al.*, 2011]. Previous workers have identified hundreds of enclosed basins with contributing valley networks, some of which appear to have overflowed and developed an outlet breach [e.g., *Forsythe and Zimbelman*, 1995; *Forsythe and Blackwelder*, 1998; *Cabrol and Grin*, 1999; *Fassett and Head*, 2008]. A small fraction of valley networks have a terminal deposit with a steep frontal scarp (summarized by *Irwin et al.* [2005] and *Hauber et al.* [2009]). These features may be relict deltas that formed in deep standing water, but some could represent aeolian deflation of fines basinward of an alluvial lag deposit, such that much of the frontal scarp relief is secondary [*Irwin et al.*, 2005]. Putative deltas and basin outlet valleys are the strongest evidence for paleolakes in the Martian highlands, but in the literature these features are rarely if ever associated with unambiguous shore landforms (e.g., shore platforms or beach ridges). Examples of highland craters with wide terraces, which may or may not be related to paleolakes, are shown in Figure 1. Some volcanic craters, such as Kilauea Iki in Hawai'i, have marginal terraces left behind when a lava lake subsided [e.g., *Holcomb*, 1971; *Tazieff*, 1994]. Large, laterally continuous terraces can also form by erosion of horizontal stratigraphy with differential resistance or through alluvial deposition at a higher base level.

[3] Previous studies have concluded that the northern lowlands, Hellas, Argyre, or large highland basins contained paleo-seas [e.g., *Parker*, 1985, 1994; *Parker et al.*, 1989, 1993, 2010; *Moore and Wilhelms*, 2001; *Irwin et al.*, 2004; *Wilson et al.*, 2010]. The basis for these interpretations includes large outlet valleys, stratified outcrops that are restricted to low elevations, or marginal platforms that may

[1]Center for Earth and Planetary Studies, National Air and Space Museum, Smithsonian Institution, Washington, D. C., USA.
[2]Planetary Science Institute, Tucson, Arizona, USA.

Corresponding author: R. P. Irwin III, Center for Earth and Planetary Studies, National Air and Space Museum, Smithsonian Institution, MRC 315, 6th St. at Independence Ave. SW, Washington, DC 20013, USA. (irwinr@si.edu)

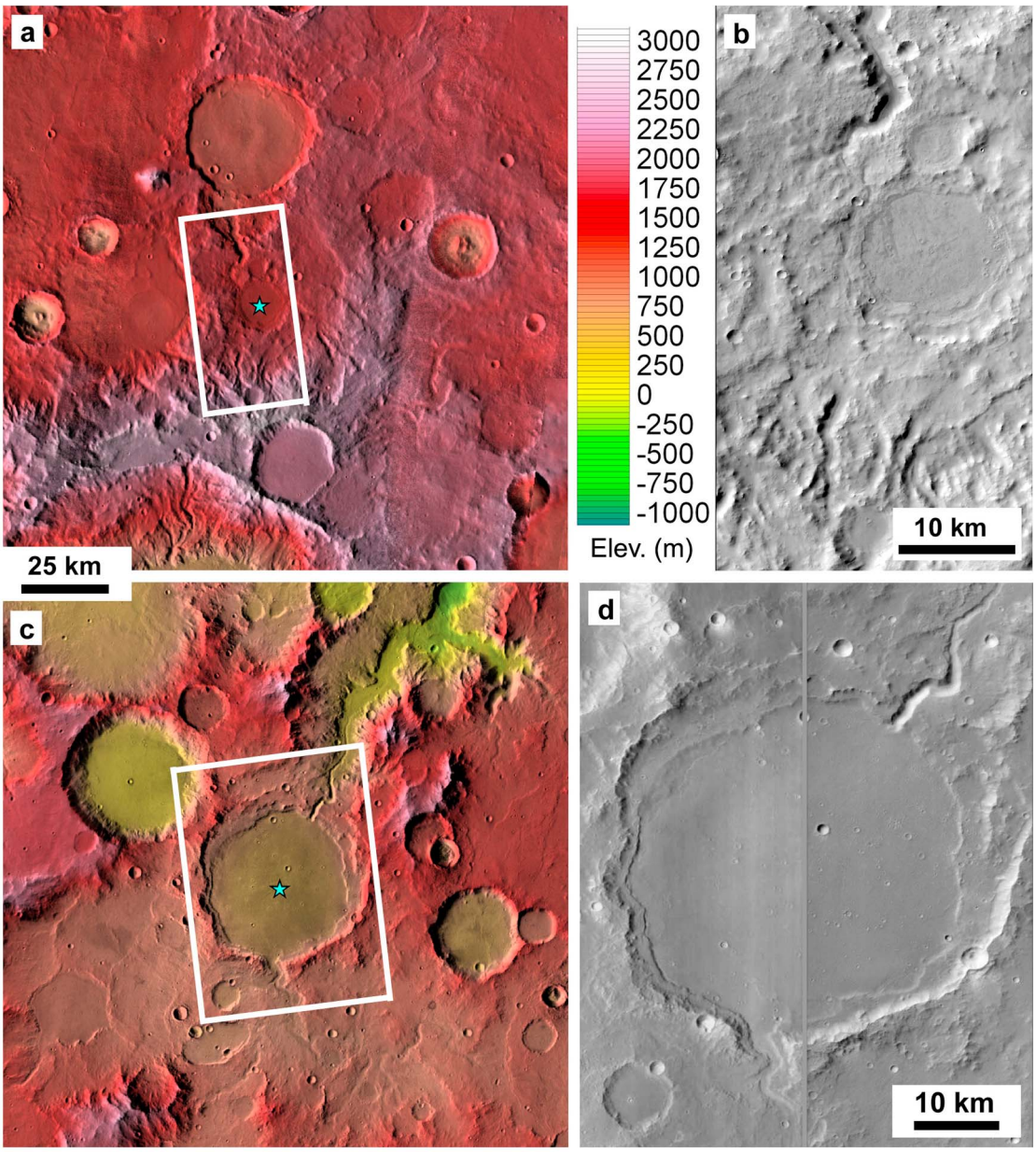

Figure 1. Two examples of Martian impact craters (marked by stars) with contributing valley networks, outlet valleys, and terraced walls. (a) A 16-km crater in southwest Arabia Terra, located at 2.17°N, 45.51°W. Mars Odyssey Thermal Emission Imaging System mosaic 2.0 colored with Mars Orbiter Laser Altimeter topography. (b) The same crater in Mars Reconnaissance Orbiter Context camera image P17_007623_1817. (c) A 46-km crater in Terra Sirenum, located at 14.63°S, 185.16°E, displayed as in 1a. (d) The same crater in Context images P11_005482_1653 and P15_006906_1655. See *Fassett and Head* [2008] for discussion of these sites.

represent strandlines. The latter features in particular have been controversial. Recent studies have tested the lowland strandlines of *Parker et al.* [1989, 1993] for topographic consistency and reproducibility in higher-resolution imaging, finding a degree of topographic irregularity and alternative interpretations for many putative shore landforms [*Head et al.*, 1999; *Malin and Edgett*, 2001; *Carr and Head*, 2003; *Tanaka et al.*, 2003; *Ghatan and Zimbelman*, 2006]. However, the relatively dense valley networks along the crustal dichotomy boundary have not been adequately explained without a source of atmospheric humidity from the lowlands [*Luo and Stepinski*, 2009; *Irwin et al.*, 2011], and the extent of lowland flooding by the Martian outflow channels is unclear but may have been significant [e.g., *Ivanov and Head*, 2001; *Carr and Head*, 2003].

[4] Theoretical investigations have shown that wave erosion of shore platforms in bedrock is possible but may be challenging under Martian conditions. Using the *Trenhaile* [2001] model for erosion of terrestrial shore platforms, *Kraal et al.* [2006] explored a range of parameter values for

slope, surf attenuation, surf threshold force for erosion, and wind speed. They found that steeper slopes, low attenuation, weak rocks, and a wind speed of 10 m/s were more favorable for erosion, given adequate time and lake level stability. If other factors are held equal, then Martian waves would be taller and have longer periods, resulting in the same time-averaged energy flux as their terrestrial counterparts. Under most conditions, surf attenuation would have limited scarp height and platform width to <10 m and <100 m, respectively. Lower atmospheric pressure [*Lorenz et al.*, 2005], persistent ice covers, and/or irregularity in the water level may have further impeded shore platform development. Previously, *Parker* [1994], *Ori et al.* [2000], *Cabrol and Grin* [2001], and *Parker and Currey* [2001] had considered the effect of lower gravity on Martian waves.

[5] Order-of-magnitude uncertainties in most of these model parameters and the likelihood that changing water levels would impede the full development of shore platforms make a terrestrial analog investigation valuable. The Great Basin study area (Figure 2) is ideal for this investigation due to the prevalent enclosed basins, relict pluvial landforms, and increasing aridity since the Late Pleistocene, all of which present a basis for comparison with early Mars. This region has long been the site of stratigraphic and hydrologic analyses of Quaternary climate change, with good chronologic control from Cascade Range tephras and radiocarbon [e.g., *Russell*, 1884; *Allison*, 1966, 1979, 1982; *Mifflin and Wheat*, 1979; *Davis*, 1985; *Hostetler and Benson*, 1990; *Benson et al.*, 1990; *Benson*, 1993; *Thompson et al.*, 1993; *Freidel*, 1993, 1994; *Cohen et al.*, 2000; *Negrini et al.*, 2000; *Licciardi*, 2001; *Huckleberry et al.*, 2001; *Zic et al.*, 2002; *Kuehn and Negrini*, 2010; *Reichert et al.*, 2011]. Moreover, recent work by *Matsubara et al.* [2011] shows that the input-evaporation balance in the pluvial Great Basin was similar to that required for observed basin outlet valleys to form by overflows on Mars. These characteristics make the Late Pleistocene paleolakes of the Great Basin a reasonable Mars analog, but the lithologic and climatic controls on their geomorphology may have differed somewhat from Mars, affecting both the sediment supply and resistance to wave erosion.

[6] *Mifflin and Wheat* [1979] concluded that the mean annual temperature in the pluvial Great Basin was only ~3°C lower than at present, given the absence of mountain glaciation over most of the Great Basin, weak weathering between drops in Lake Lahontan's level, lack of ice-marginal features near the highstand, presence of tufa deposits, and aquatic faunal and palynological evidence suggesting little change in temperature. Other workers have suggested pluvial temperatures 5–10° cooler than at present [e.g., *Thompson et al.*, 1993]. Movement of the polar jet stream in response to advance and retreat of the Laurentide ice sheet is thought to be mostly responsible for climate change in the region [e.g., *Antevs*, 1948; *Hostetler and Benson*, 1990; *Oviatt*, 1997; *Negrini et al.*, 2000]. More favorable storm tracks were likely responsible for lake development, bringing substantially more winter precipitation into the area. Relationships between sedimentary indicators of lake level and magnetite concentrations over a 250,000-year stratigraphic section in Summer Lake, Oregon [*Negrini et al.*, 2000; *Cohen et al.*, 2000] suggest that higher-frequency fluctuations are driven by an atmospheric response to changes in North Atlantic sea surface temperature [*Zic et al.*, 2002].

[7] Within the study region, satellite image mosaics from Google Maps (http://maps.google.com) were used to choose survey locations in five enclosed basins: Spring Valley, Long Valley, and Surprise Valley in Nevada; and Christmas Valley and Summer Lake basin in Oregon (Figure 2). These sites collectively contain prominent erosional platforms, depositional beach ridges, and relict fan-deltas. This paper focuses on erosional shore platforms in Oregon; *Ghatan and Zimbelman* [2006], *Zimbelman and Irwin* [2008], and *Zimbelman et al.* [2009] describe beach ridges in Nevada in more detail.

[8] Christmas Valley and the adjacent Summer Lake basin are irregularly shaped, down-faulted basins bordered mostly by fault scarps, tilted blocks, and volcanic surfaces (Figure 3). The bedrock geology is mostly flows and tuffs of Tertiary basalt and andesite, with Quaternary volcanics bordering Christmas Valley to the north [*Walker and MacLeod*, 1991]. Aeolian reworking of devegetated surfaces on the basin floors has formed deflation pans and dune fields. The climate is characterized by low precipitation of 10–35 cm/y (averaging 32 cm/y) and temperature extremes of −40 to +43°C (averaging 9°C) [*Allison*, 1966, 1982; *Reichert et al.*, 2011]. *Freidel* [1993] noted a strong gradient in precipitation between the western (70–80 cm/y) and eastern (<25 cm/y) contributing watersheds.

[9] *Russell* [1884, 1905] provided early descriptions of these two paleolakes, and *Meinzer* [1922] and *Snyder et al.* [1964] mapped their extent. The most comprehensive studies of shore landforms in Christmas Valley and the Summer Lake basin are by *Forbes* [1973], *Allison* [1979, 1982], and *Freidel* [1993]. Shore landforms at discrete locations around both basins (pluvial lakes Fort Rock and Chewaucan, respectively) include erosional platforms, scarps, and caves; as well as terraces, beach ridges, spits, and deltaic deposits of rounded gravel and finer-grained sediment. These prior workers identified three main stillstands in Christmas Valley: 1364–1366 m, 1353–1356 m, and 1332 m. A large beach ridge at 1384 m likely predates the last filling episode. The main stillstands in the Summer Lake basin were 1370–1372, 1364–1367, and 1358–1359 m. Brecciated normal faults striking NW–SE convey groundwater from Christmas Valley into the Summer Lake basin and may have provided a degree of hydrologic integration the past [*Freidel*, 1993]. Radiocarbon ages suggest that these lakes occupied their highstands at least 18,000 to 16,400 radiocarbon years before present.

[10] The present study addresses three issues regarding shore landforms on Mars: 1) the scale and morphology of common landforms along terrestrial paleolake shorelines, 2) the data products that would be needed to identify these landforms in pristine condition on Mars, and 3) the potential of these features to survive post-Noachian degradation. Critical analysis of putative shore landforms identified in prior literature (including around the largest Martian basins) and generation of data products for this purpose are beyond the scope of this project, but the results presented here would facilitate that future work. Precise field-surveyed topographic data from Late Pleistocene Great Basin shorelines in Oregon

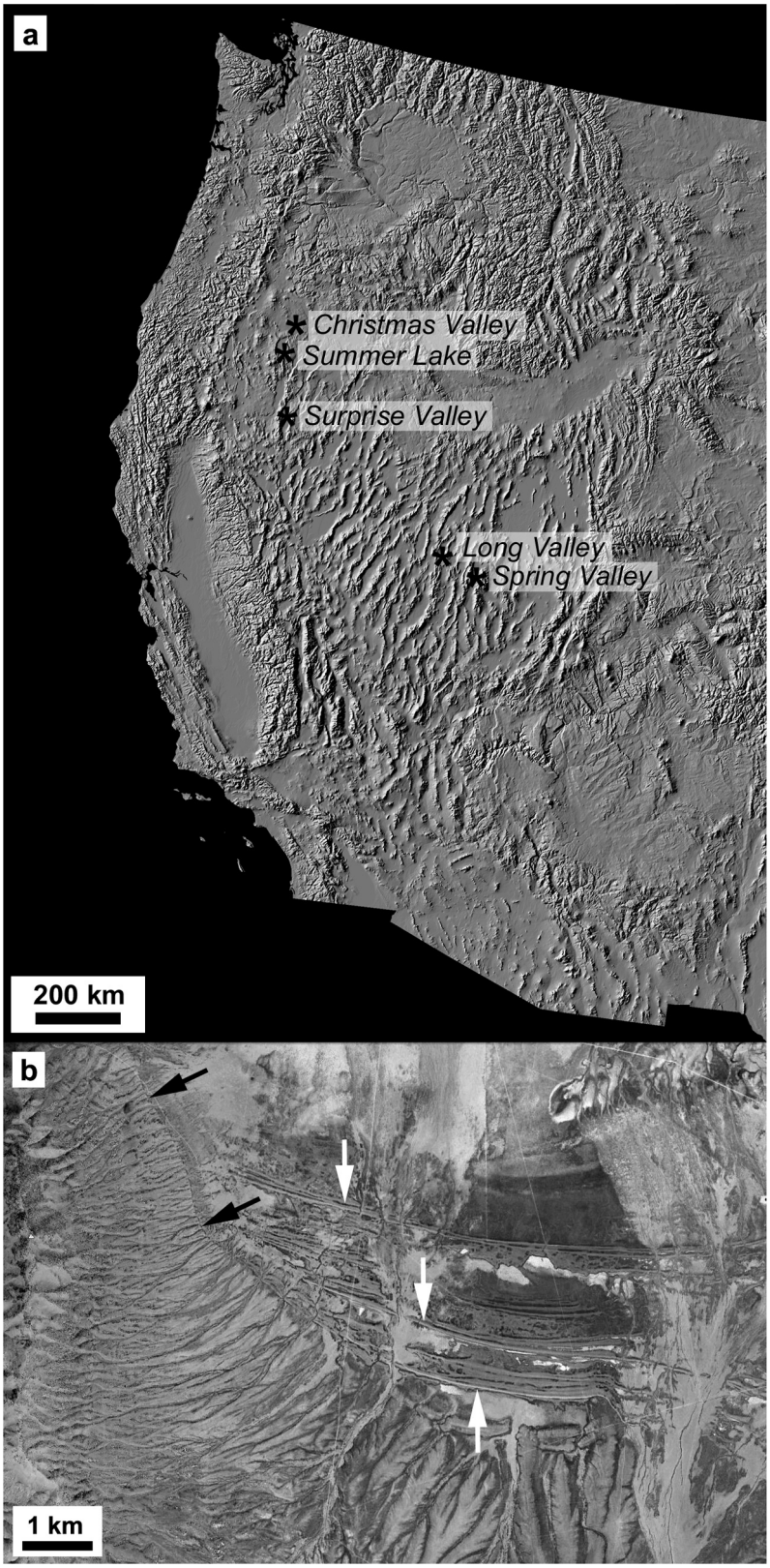

Figure 2. (a) Locations of the five pluvial lake basins included in this study. Shaded relief base map of the western United States after *Thelin and Pike* [1991]. (b) An erosional scarp (black arrows) and depositional beach ridges (white arrows) in southwestern Long Valley, Nevada. The scarp base is at the elevation of the highest beach ridge (lower white arrow). Google Earth Imagery ©Google Inc. and U.S. Department of Agriculture Farm Service Agency. Used with permission.

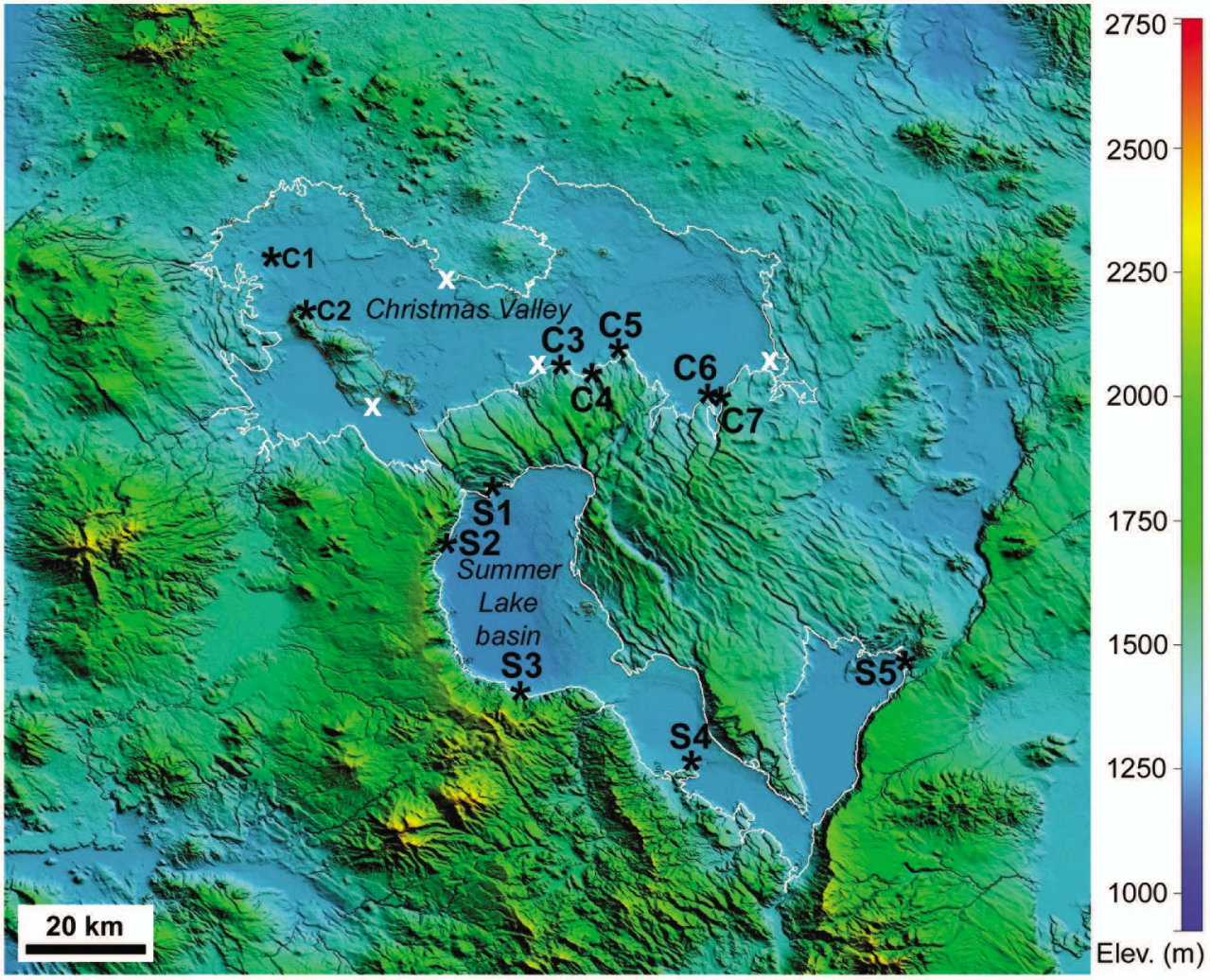

Figure 3. Study area in south-central Oregon showing the locations of survey profiles relative to the 1367 m contour (white line). Survey locations are marked with an asterisk and number. Survey sites that were interpreted with less confidence are marked with a white X and not included in the tables. National Elevation Data set at 30.9 m/pixel resolution, bounded by 43.75°N, 42.28°N, 121.27°W, and 119.83°W.

and Nevada, U.S.A., provide the necessary scale information. We compare these results to long-term denudation rates and the resolution of available Mars data products for insight into preservation and detection issues, respectively. Field observations of erosional and depositional shore landforms and a comparison of multiple survey lines within each basin provide additional insight into anticipated conditions on Mars.

2. Methods

[11] On four trips between 2008 and 2011, differential Global Positioning System (DGPS) survey data and other field observations were collected at 54 locations within the five basins. We used a Trimble R8 Differential Global Positioning System (DGPS) instrument, which typically has single-digit precision at centimeter scales in both horizontal and vertical dimensions, relative to a tripod-mounted base station (described by *Zimbelman and Johnston* [2001]). We placed each base station near either a U.S. Geological Survey (USGS) benchmark or a USGS-surveyed road intersection where no benchmark was available, and we surveyed these known points for absolute elevation control of ~0.3–1 m. Our survey data and inferred lake levels are only as accurate as the USGS surveys, as shown on 1:24,000 USGS topographic maps. We converted the DGPS survey data (easting, northing, and elevation) to topographic profiles that allow precise measurements of the shore landform dimensions and elevations. To discriminate shore landforms from other profile irregularities, we identified features in the field with lateral continuity for hundreds of meters along a contour line, and we noted the survey point numbers as we crossed those features. This method was effective, as the volcanic bedrock in this area is typically not flat-lying.

[12] Digital elevation models (DEMs) were available at resolutions of 1 arcsecond (30.9 m) per pixel from the USGS-maintained National Elevation Data set (NED) (http://seamless.usgs.gov/) and the Shuttle Radar Topography Mission (SRTM) (http://eros.usgs.gov/#Find_Data/Products_and_Data_Available/SRTM). In the former, grid cells are not interpolated between

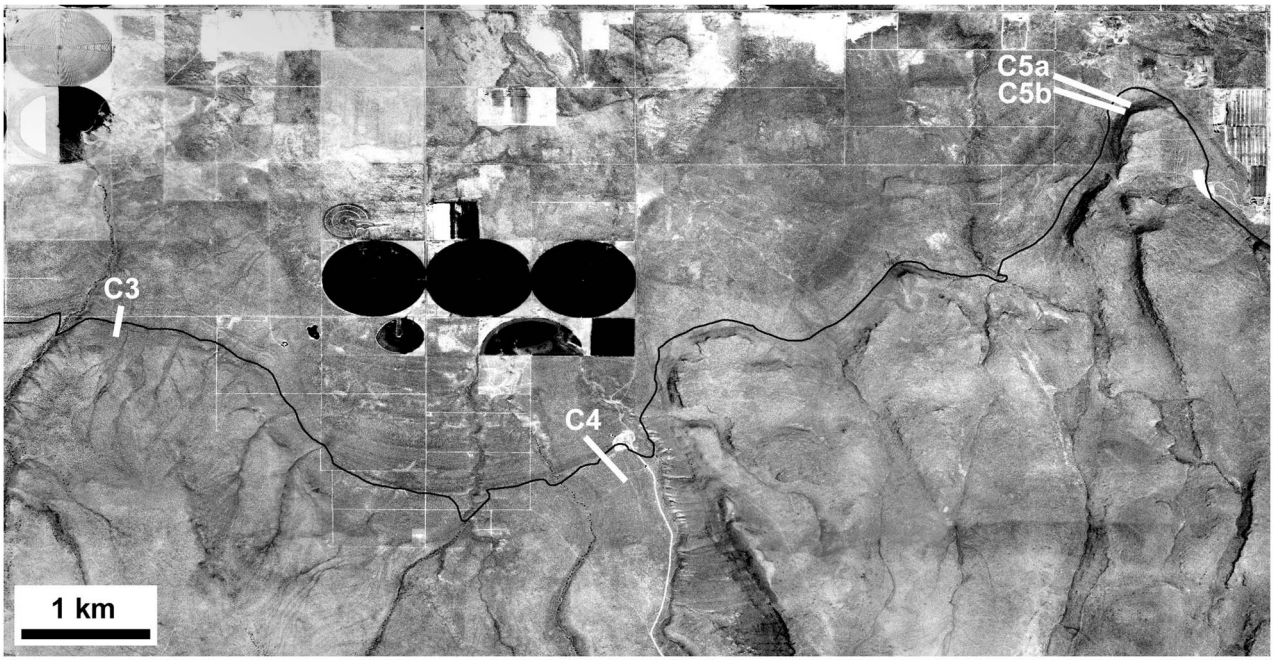

Figure 4. Interpretation of the Fort Rock paleolake's Late Pleistocene highstand, Christmas Valley, using DOQ data. The 1366 m contour line is shown in black, and white lines are survey profiles numbered as in Figure 3.

contour lines, giving the data set a stair-stepped appearance, particularly on gentle slopes. This characteristic is inconvenient for identifying shore landforms in the topography. The SRTM data have a rough appearance near the limit of resolution, which also complicates identifying and determining the elevation of shore landforms using topographic data alone. For these reasons, we used the DEMs for basin-scale measurements and context, and we relied on the DGPS for precise local measurements. For comparison, the Mars Orbiter Laser Altimeter (MOLA) topographic grid has a resolution of 463 m/pixel near the equator. High Resolution Stereo Camera (HRSC) digital elevation models from the Mars Express mission are available for much of Mars with resolutions of up to 50 m/pixel (more comparable to the NED) and elevation accuracy up to 10 m [*Jaumann et al.*, 2007]. Stereo DEMs derived from the High Resolution Imaging Science Experiment (HiRISE) on the Mars Reconnaissance Orbiter are as fine as 1 m/pixel and more similar to the DGPS data in scale [e.g., *Kirk et al.*, 2008].

[13] Some Great Basin paleolakes, such as Lake Bonneville, maintained one or more major levels for longer periods due to control by an outlet, under conditions where input exceeded evaporation from the lake [e.g., *O'Connor*, 1993]. Lake Bonneville had stabilized at the Bonneville level before the Bonneville Flood, when the outlet was rapidly downcut, and it occupied the lower Provo level for some time thereafter, both controlled by the elevation of the outlet. These circumstances allowed development of the two most prominent shore platforms around Lake Bonneville. We used the NED DEMs to test the hypothesis that an outlet controlled the level of the five paleolakes described here. To determine the overflow elevation of each basin, we used Rivix RiverTools 3.0 software to fill all enclosed basins to their respective overflow points and produce a DEM with integrated drainage. In this processed DEM, every pixel within an enclosed basin is raised to the elevation of the outlet. Extracting the river network from this processed DEM indicates where the putative outlet would have been, and we examined these locations for evidence of incision.

[14] To determine whether each paleolake reached its overflow point, we downloaded digital orthophoto quads (DOQs) with 1 m/pixel resolution for each basin from the Oregon Geospatial Enterprise Office (http://www.oregon.gov/DAS/EISPD/GEO/data/doq.shtml) and the University of Nevada at Reno's W.M. Keck Earth Sciences and Mining Research Information Center (http://keck.library.unr.edu/Data/DOQ). We overlaid these map-projected data onto the NED using Global Mapper 9.0 software, and we generated contours at multiple levels to identify one that best reflects the observed highstand in the imaging (Figure 4). We examined the perimeter of the basin at this contour line for consistency. Typically we were able to constrain the highstand to $\pm$1–2 m, but uncertainty in the steep-walled Summer Lake basin was closer to $\pm$5 m. We also compared these estimates to strandline elevations that we surveyed in the field, in order to determine whether the field surveys captured the highstands.

[15] We determined the maximum area of each paleolake by creating a vector shapefile of the highstand contour line, converting it to an enclosed polygon, and calculating the area using ESRI ArcGIS 9.3 software. Drainage basin areas came from the Nevada State Engineer Basin Boundaries data set (http://water.nv.gov/mapping/gis/) and the Pacific Northwest Hydrography Framework's Watershed Boundary Data set (http://www.pnwhf.org/water-bound-dataset.aspx). For Surprise Valley, which extends into California, we used Global Mapper to plot a polygon over the drainage divides as seen in the NED and calculate the polygon's area.

Table 1. Paleolake Highstand, Pour Point, Lake Area at Highstand, and Watershed Area

Valley	Paleolake[a]	Highstand Elevation (±2 m)	Pour Point Elevation (m)	Lake Area, Highstand (km^2)	Watershed Area (km^2)	Watershed Area/Lake Area
Christmas	Fort Rock	1366	1436	1918	6963	3.6
Summer	Chewaucan	1372 ± 5	1448	1233	3366	2.7
Surprise	Surprise	1545	1621	1430	3837	2.7
Long	Hubbs	1910	1949	467	1699	3.6
Spring N	Spring	1759	1850[b]	619	4318[c]	5.4[c]
Spring S	Maxey	1766	1850[b]	180	4318[c]	5.4[c]

[a]Paleolake names from *Mifflin and Wheat* [1979] and *Reheis* [1999].
[b]At the 1850 m pour point, the northern and southern paleolakes in Spring Valley would have been integrated.
[c]Paleolake Maxey drained into Paleolake Spring. These numbers represent the total watershed area in Spring Valley (north plus south) and the total paleolake area (Spring plus Maxey).

[16] To compare these erosional features to fully developed shore platforms, we used the theoretical maximum platform widths from *Trenhaile* [2001] and *Kraal et al.* [2006]. We estimated the scale of features that could be preserved from three geologic epochs early in Martian history using post-Hesperian denudation rates from *Golombek et al.* [2006], estimates of impact gardening from *Hartmann et al.* [2001], and comparison to the size of craters that have survived since the Noachian [*Hartmann*, 2005].

3. Results

3.1. Lake Levels and Maintenance of Endorheic Drainage

[17] Table 1 shows the Late Pleistocene highstand elevation, basin pour point elevation, paleolake area at the highstand, and watershed area for the five basins in this study, determined using the methods described above. Tables 2 and 3 compare these results to prior work. Our highstand estimate is the same as that of *Reheis* [1999] for Spring Valley. In the Paleolake Maxey subbasin in southern Spring Valley, we found an overflow level of 1766 m, which compares to 1762 m from *Reheis* [1999] and 1792 m from *Mifflin and Wheat* [1979]. In Long and Surprise Valleys, we found levels that were 10 and 22 m respectively below the published values of *Mifflin and Wheat* [1979]. In Christmas Valley and the Summer Lake basin, our highstand estimates are consistent with those of *Freidel* [1993], and maximum lake area measurements were within 2% of those estimated by *Freidel* [1993] and *Licciardi* [2001], respectively.

[18] We conclude that none of these five paleolake basins overflowed during the timescale represented by their surveyed shore landforms (Table 1), as their highstands were 39–91 m below their overflow points (as defined by analysis of the DEM in RiverTools), and the outlets showed no evidence of dissection, at least during the last glacial maximum. This result is consistent with prior work by *Mifflin and Wheat* [1979], who interpreted that these basins maintained endorheic drainage during the most recent episode of infilling.

3.2. Dimensions of Pluvial Shore Landforms

[19] Measurements of shore landforms were taken from the DGPS data as described above. Figure 5 shows three example survey profiles of erosional shore platforms, one from Christmas Valley and two from the Summer Lake basin. The lake level is interpreted to be the point of maximum concavity (upper edge of the platform) for erosional shore platforms, the convex break in slope at the outer edge of depositional surfaces, and half the height of a beach ridge. Platform widths are the distance between the upper and lower margins of the platform as recorded in the survey data and field notes. Where we surveyed an erosional scarp with a long slope rather than a narrower platform at its base, we report the strandline elevation as a possible range rather than an integer value, and we do not report a width. For example, in three areas in the Summer Lake basin, we surveyed scarps between ~1366 and 1378 m. *Allison* [1982, p. 64] interpreted 1378 m as the highstand based on evidence at other locations, whereas the base of the scarps at 1367 m was "a sustained… level marked by pronounced beach development." *Freidel* [1993] could not find evidence for a strandline at 1378 m and interpreted 1372 m as the highstand, with other prominent stillstands at 1364–1367 and 1358–1359 m.

[20] Platform widths vary over an order of magnitude between 2 and 25 m, but individual strandlines are not this well expressed around the entire perimeter of the basins (Table 4). Strandlines with prominent terraces in one location may have none at another, even when the two sites are within a few kilometers of each other. For example, in Christmas Valley, shore landforms are discontinuous and only evident along the southern side of the basin [see also *Freidel*, 1993]. Some water levels (generally ~1366, 1356,

Table 2. Paleolake Highstands From This Study Compared With Previous Work

Valley	Paleolake[a]	Highstand Elevation (±2 m)	Published Highstand Elevation (m)	Reference
Christmas	Fort Rock	1366	1364–1366	*Freidel* [1993]
Summer	Chewaucan	1372±5	1370–1372	*Freidel* [1993]
Surprise	Surprise	1545	1567	*Reheis* [1999]
Long	Hubbs	1910	1920	*Reheis* [1999]
Spring N	Spring	1759	1759	*Reheis* [1999]
Spring S	Maxey	1766	1762	*Reheis* [1999]

[a]Paleolake names from *Mifflin and Wheat* [1979] and *Reheis* [1999].

Table 3. Paleolake and Watershed Areas From This Study Compared With Previous Work

Valley	Lake Area, Highstand (km^2)	Published Lake Area, Highstand (km^2)	Watershed Area (km^2)	Published Watershed Area (km^2)	Watershed Area/Lake Area	Published Watershed Area/Lake Area
Christmas	1918	1946[a]	6963	7535[a]	3.6	3.9
Summer	1233	1247[a]	3366	3785[a]	2.7	3.0
Surprise	1430	1471	3837	4040	2.7	2.7
Long	467	505	1699	1725	3.6	3.4
Spring N	619	603	4318[b]	4291[b]	5.4[b]	5.3[b]
Spring S	180	210	4318[b]	4291[b]	5.4[b]	5.3[b]

[a]Source: *Freidel* [1993]. Other published data are from *Mifflin and Wheat* [1979].
[b]Paleolake Maxey drained into Paleolake Spring. These numbers represent the total watershed area in Spring Valley (north plus south) and the total paleolake area (Spring plus Maxey).

and 1346 m) have evident shore landforms in multiple survey lines but not all. Where the top of a survey line is below the inferred highstand, it was because a higher shore platform was not visible at that location.

[21] For comparison, we surveyed beach ridges at 13 locations, two of which are in Christmas Valley. In the example shown in Figure 6, beach ridges are <1 m high and <100 m wide, but more than a kilometer long. These depositional features are evident in the field but subtle, particularly where a scrubby cover of vegetation is present. *Ghatan and Zimbelman* [2006], *Zimbelman and Irwin* [2008], and *Zimbelman et al.* [2009] discuss these and other Late Pleistocene beach ridges in more detail.

3.3. Equilibrium Dimensions of Shore Platforms

[22] A motivating issue for this study is that theoretical investigations of shore platform dimensions include large uncertainties in several key parameter values, such that it is not clear how large erosional shore platforms on Mars should be. *Trenhaile* [2001] modeled the erosion of shore platforms under a range of conditions, with parameters constrained where possible by field data. *Kraal et al.* [2006] examined the parameter space to estimate the maximum size of shore platforms under a range of conditions. Width is limited by attenuation of wave energy on the platform, such that little energy is available to attack the base of the scarp. The most relevant model result used moderate values for the critical surf force for erosion, attenuation of wave energy on the platform, and wind speed, while varying slope at 1°, 5°, 10°, and 20°. Erosional scarps and platforms did not form at 1°, whereas maximum widths were approximately 23 m, 45 m, and 55 m at 5°, 10°, and 20°, respectively [*Kraal et al.*, 2006, Figure 5]. Our measurements are consistent with their development of scarps and shore platforms only on steeper slopes, whereas beach ridges are limited to gentle slopes of <1–2° at both the Oregon (Table 5) and Nevada field sites.

[23] The surveyed shore platforms vary in width over an order of magnitude from 2 to 25 m. At some locations, we surveyed platforms of significantly different width on individual slopes, where the lithology appeared similar up-section. None of the surveyed platforms reached the maximum widths of tens to hundreds of meters that *Trenhaile* [2001] and *Kraal et al.* [2006] estimated could form under favorable long-term conditions. Although maximum widths can be limited to the range observed here under certain combinations of parameter values (for a given slope, this could be a rough surf zone, strong bedrock, and/or less effective wind velocity), we interpret that most or all of the surveyed shore platforms are underdeveloped due to limited fetch and time that the paleolakes maintained each level.

4. Discussion

4.1. Development of Pluvial Shore Landforms

[24] Observations of shore landforms in a terrestrial analog setting will not solve longstanding questions over the occurrence and distribution of paleolakes on Mars, but they are useful in guiding the investigator on what to look for, where to look, how observations may be interpreted, and how the available data products may be useful. As we suggest below, shore landforms of this size are unlikely to have survived since the early wetter epoch(s) on Mars, except perhaps under special circumstances.

[25] Most pluvial shore platforms and beach ridges in the Great Basin are topographically subtle features, up to meters high and meters to a few tens of meters wide. Depositional beach ridges on low gradients are particularly low in relief, and prominent in plan view imaging largely due to differences in vegetation and filling of topographic lows with fine-grained sediment (Figures 4 and 6). For this reason, they are easier to identify in plan view imaging than in the field. Part of the size limitation may be related to variable lake levels in closed basins, but attenuation of wave energy on shore platforms also limits their development. Water bodies with a longer fetch, more stable water levels, and more erodible materials can develop shore platforms an order of magnitude larger [*Trenhaile*, 2001], but these ideal conditions may not have been common in enclosed basins on early Mars. Larger depositional landforms like those found along terrestrial marine coasts are also possible on Mars, but they are not expected in the smaller highland basins of interest here. Lakes with fetch <50 km typically have limited wave energy, so lithology, currents, and ice may have relatively important roles inshore landform development. Shorelines with irregular planform have variable exposure to waves, smaller beaches and bars, and beach materials derived from local source rocks [*Nordstrom and Jackson*, 2012].

[26] The ratio of drainage basin area (including the lake) to maximum paleolake area varied from 2.7 to 5.4 among the five studied basins. *Fassett and Head* [2008] reported watershed/paleolake area ratios for 73 paleolakes that appeared to have overflowed on Mars, but only 13 fell within this range or had lower ratios, and many of them were inferred to have substantial contributions from regional groundwater. If the paleoclimate around the Noachian/Hesperian transition on Mars were similar to the Great Basin pluvial paleoclimate, at

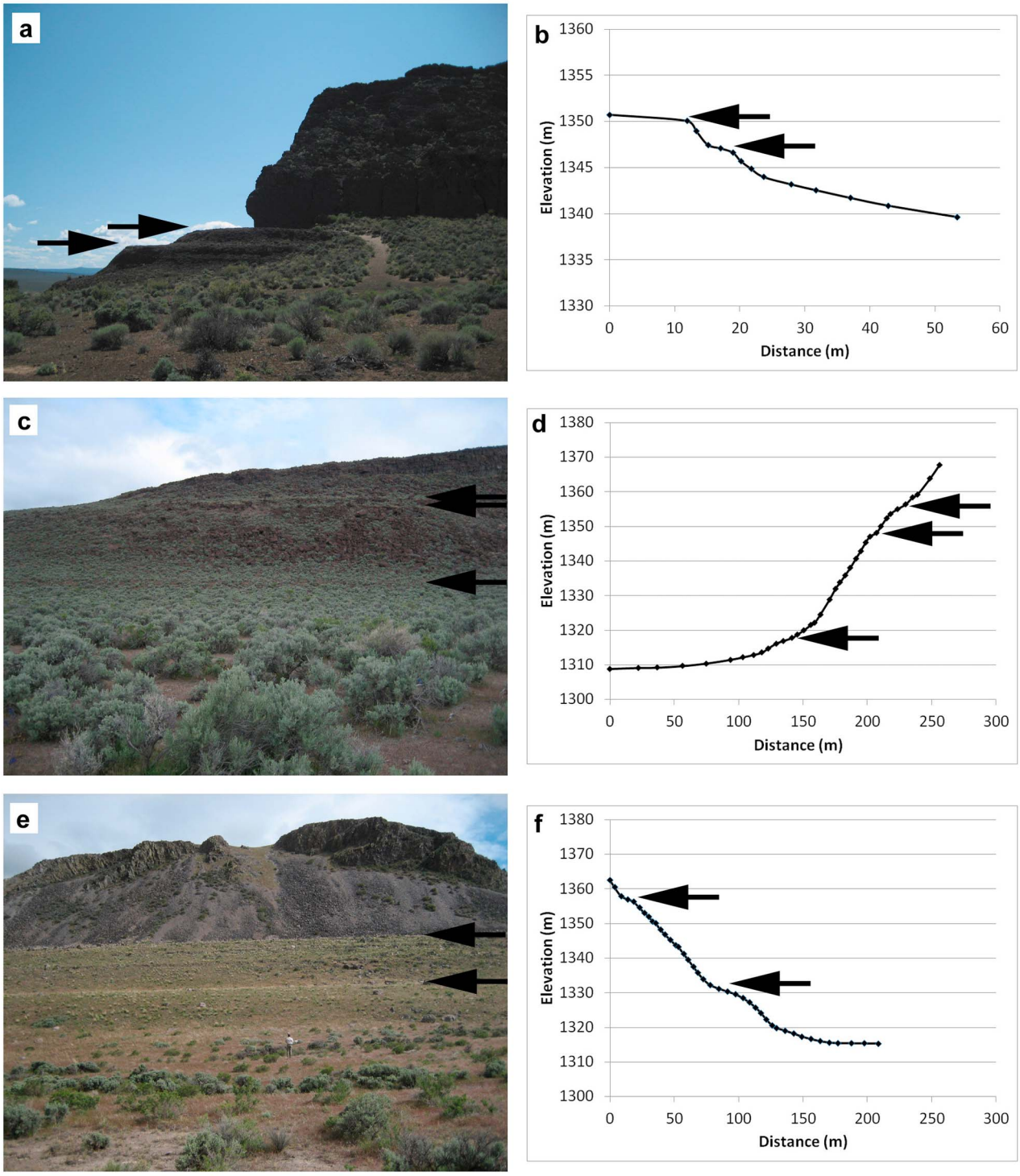

Figure 5. Erosional shore platforms, marked by arrows. (a, b) Site C1, Fort Rock in Christmas Valley. Profile runs west–east from left to right. (c, d) Site S1 in the Summer Lake basin. Profile runs south–north. (e, f) Site S4b in the Summer Lake basin. Profile runs south–north. The survey profiles shown at right plot approximately through the middle of each image.

least as an upper bound, then simple geometric relationships suggest that impact craters could have maintained lakes that were 43% to 61% of the crater diameter. The maximum depth of the lake would depend on the geometry of the impact crater, with shallower lakes in flatter-floored craters, unless a water source from outside the crater were available. In many craters without contributing drainage from outside, the lake would be confined to the crater floor and would not onlap the wall. These considerations suggest that many crater paleolakes (particularly ones without exterior contributing

Table 4. Interpreted Lake Levels and Shore Platform Widths in Christmas Valley and the Summer Lake Basin Based on DGPS Survey Data.

Valley	Profile	Elevation Range of Profile (m)	Level 1 Elevation (Width) (m)	Level 2 Elevation (Width) (m)	Level 3 Elevation (Width) (m)	Level 4 Elevation (Width) (m)
Christmas	C1	1340–1351			1350, 1347 (11, 4)	
Christmas	C2	1346–1375	1367 (N/A)[a]			
Christmas	C3	1355–1370	1363–1366 (N/A)[b]			
Christmas	C4	1356–1371	1364 (N/A)[a]	1360, 1358 (N/A)[a]		
Christmas	C5a	1330–1382	1364–1367 (N/A)[b]	1357–1361 (N/A)[b]	1348–1350 (N/A)[b]	
Christmas	C5b	1332–1382	1359–1367 (N/A)[b]		1345–1346 (N/A)[b]	
Christmas	C6a	1316–1368		1356 (8)		
Christmas	C6b	1317–1374		1356 (5)		
Christmas	C7a	1334–1363		1356 (17)		
Christmas	C7b	1333–1360		1356 (9)	1346? (7)	
Christmas	C7c	1329–1335				1331, 1333, 1334 (N/A)[a]
Summer	S1a	1309–1367		1355 (12)	1348 (5)	1318? (12)
Summer	S1b	1341–1348			1348 (27)	
Summer	S2	1301–1395	1369–1378 (N/A)[b]			1337–1339 (N/A)[b]
Summer	S3	1321–1380	1366–1377 (N/A)[b]	1354–1356 (N/A)[b]	1344–1347 (N/A)[b]	1325–1335 (N/A)[b]
Summer	S4a	1315–1363		1358 (11)	1351, 1344 (5), (3)	1332 (24)
Summer	S4b	1315–1363		1358 (10)	1351, 1344 (3), (2)	1332 (25)
Summer	S5a	1347–1374	1366, 1369 (N/A)[b]			
Summer	S5b	1349–1379	1367–1378 (N/A)[b]			
Summer	S5c	1354–1384	1368–1377 (N/A)[b]			

[a]Feature is depositional.
[b]Higher number applies if feature is depositional.

drainage) may never have developed shore landforms on their walls. Depositional beach ridges or other shore landforms may have developed on low-gradient crater floors, but these features are often more subtle in relief.

[27] We find that individual strandlines are often not equally well expressed around the entire perimeter of a basin. In some survey locations, the highstand is indistinct, but a level 10 m lower is clearly expressed. That lower level may be indistinct elsewhere. This issue may be due to the variable susceptibility of bedrock to wave erosion, and fetch in the dominant wind direction may lead to more energetic wave attack in some locations than others [e.g., *Freidel*, 1993]. Undermining very steep surfaces can trigger mass wasting from above, such that a platform never develops, and low slopes may form depositional rather than erosional features. It is therefore problematic to identify isolated topographic steps or terraces using plan view imaging alone and interpret connections between them. Moreover, a lack of topographic consistency between observed platforms or terraces is not conclusive evidence that they are not shore landforms, because the observed features may have formed at different times.

4.2. Preservation and Detection

[28] Preservation of shore landforms against later impact gardening and aeolian erosion may be the greatest challenge with respect to identification on Mars using orbital data sets. The potential to preserve small landforms on Mars depends strongly on age. Margaritifer Terra, for example, has lost nearly all of its Noachian craters <8 km in diameter and all

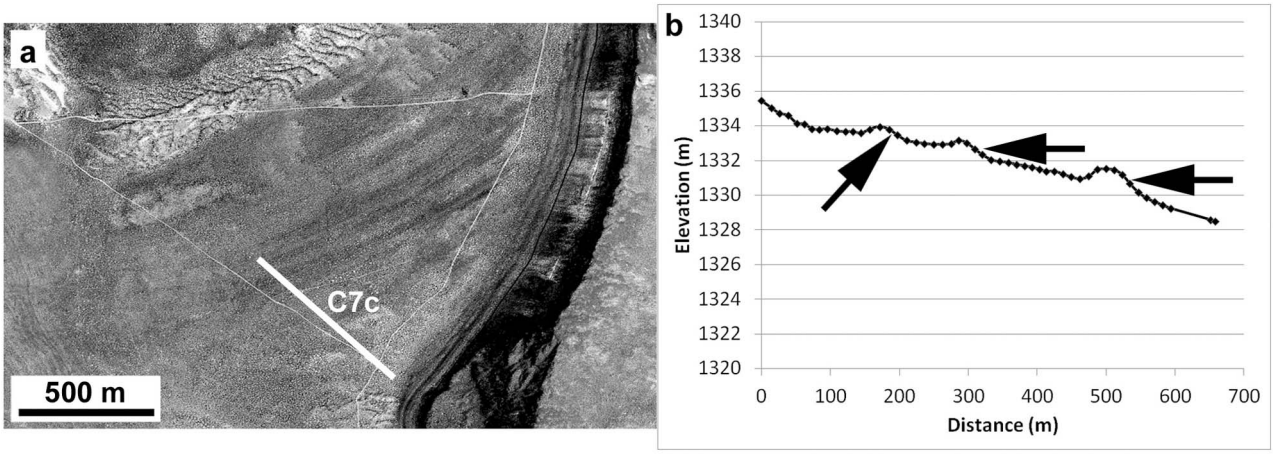

Figure 6. Beach ridges at site C7 in eastern Christmas Valley. (a) DOQ base mosaic. (b) Profile C7c, indicated by the white line in (a), surveyed from SE to NW. Note the low relief of the beach ridges despite their prominence in imaging.

Table 5. Shore Platform Widths and Slope of the Surface Into Which They Are Incised

Valley	Profile	Elevation Range (m)	Mean Slope (°)	Elevation of Widest Platform (Width) (m)
Christmas	C1	1344–1350	27.3	1350 (11)
Christmas	C2	1346–1375	3.9	N/A (delta)
Christmas	C3	1355–1370	2.7	N/A (scarp)
Christmas	C4	1356–1371	1.5	N/A (beach ridges)
Christmas	C5a	1341–1378	5.1	N/A (scarps)
Christmas	C5b	1339–1376	5.0	N/A (scarps)
Christmas	C6a	1330–1368	20.6	1356 (8)
Christmas	C6b	1328–1371	23.2	1356 (5)
Christmas	C7a	1338–1363	13.7	1356 (17)
Christmas	C7b	1341–1360	13.6	1356 (9)
Christmas	C7c	1329–1334	0.5	N/A (beach ridges)
Summer	S1a	1322–1367	25.1	1355 (12)
Summer	S1b	1341–1348	N/A	1348 (27)
Summer	S2	1327–1395	10.9	N/A (scarps)
Summer	S3	1325–1377	9.3	N/A (scarps)
Summer	S4a	1320–1363	18.0	1332 (24)
Summer	S4b	1321–1363	18.5	1332 (25)
Summer	S5a	1347–1373	3.2	N/A (scarps)
Summer	S5b	1349–1379	N/A	N/A (scarp)
Summer	S5c	1354–1384	8.3	N/A (scarp)

of those <4 km [*Hartmann et al.*, 2001; *Irwin and Grant*, 2012], implying that other Noachian landscape elements of that scale or smaller would not have survived, unless they were actively maintained. Moreover, *Hartmann et al.* [2001] estimated that 14–25 m of impact gardening has occurred since the last major resurfacing of Margaritifer Terra. The *Hartmann* [2005] isochrons imply saturation at diameters below ~200 m for surfaces that are 3.5 Gy old (Early Hesperian), a reasonable estimate for intercrater plains in that area. Rover observations confirm this result. At the Mars Exploration Rover (MER) Spirit landing site, Hesperian basalts were gardened to depths of at least 10–20 m [*Greeley et al.*, 2005; *Grant et al.*, 2006; *Golombek et al.*, 2006]. This amount of impact gardening should make Noachian to Early Hesperian features of the scale surveyed here indistinct in imaging and topography. Small deltaic deposits, such as the one surveyed in western Christmas Valley (Figure 7), would also not have survived impact gardening at this scale.

[29] The setting of shore landforms is another factor in their preservation. Depositional beach ridges may be topographically subtle, unconsolidated, and finer-grained than erosional shore platforms, making them susceptible to aeolian burial or erosion beyond the effect of impact gardening. Erosional shore platforms can be larger but are often located on steeper slopes, which can be susceptible to mass wasting. Small impacts may facilitate slope processes on Mars, making the effect of impact gardening greater on steep slopes.

[30] Despite these adverse circumstances, a focused search for shore landforms could be worthwhile in some locations. They should be best expressed in climates that are cool enough for perennial lakes to form but not so cold that ice cover inhibits wave action. Elevation control (such as by a surface outlet) or a stable water supply relative to evaporation would be useful for focusing wave action at one or more consistent levels (this consideration also applies to deltas). Large features and late hydrologic activity are essential to avoid complete loss to impact gardening. *Grant and Wilson* [2011] showed that in the Margaritifer Terra region, development of deltas and fans continued from the Late Hesperian into the Early Amazonian Epochs, which may account for the excellent preservation of fluvial sedimentary structures relative to most other depositional basins on Mars.

[31] Identifying shore landforms of the scale described here would require imaging and topographic products of meter to submeter resolutions. Gridded or shot data from MOLA [*Smith et al.*, 2001] would be inadequate to detect any of the features studied here, as would imaging of >10 m/pixel resolution. Imaging of ~1–5 m/pixel, including Mars Orbiter Camera or Context Camera data, could be useful in some locations at the native resolution of the imaging, but stereo DEMs derived from those images have lower resolution. At present, the best prospect would be imaging and stereo DEMs from HiRISE [*McEwen et al.*, 2007; *Kirk et al.*, 2008], targeted to basins that received water from Late Hesperian to Amazonian, extensive fluvial networks. However, contrasts in vegetation cover make the terrestrial shore landforms

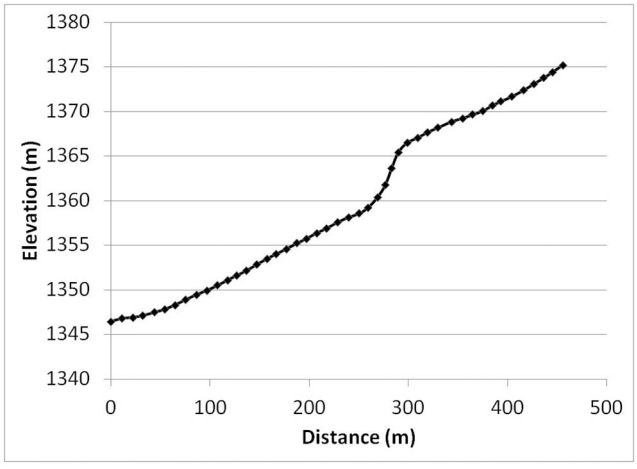

Figure 7. Profile of an alluvial deposit that is graded to a base level at or below 1367 m and may have been undercut at lower lake levels. Site C2 in western Christmas Valley. The lake was to the left (east) in this profile.

much more obvious in imaging, whereas contrast on the Martian surface is low and would make detection more difficult relative to the terrestrial field areas described here.

5. Conclusions

[32] Highland basins with contributing valley networks, outlet valleys, and/or deltas present strong evidence for paleolakes on Mars [e.g., *Cabrol and Grin*, 1999; *Irwin et al.*, 2005; *Fassett and Head*, 2008], and seas have been suggested in other large basins [e.g., *Parker et al.*, 1989; *Moore and Wilhelms*, 2001]. However, shore landforms are often ambiguous or absent in all of these settings [e.g., *Malin and Edgett*, 2001; *Ghatan and Zimbelman*, 2006]. High-precision DGPS topographic surveys of erosional shore platforms and depositional beach ridges in the Great Basin region provide estimates of the size of landforms that might have formed in highland basins on Mars. We compared these measurements to published theoretical maxima and to the scale of features that have survived since early Martian history for insight into whether shore landforms might have remained preserved until the present.

[33] For the five field areas, our interpreted highstands and paleolake areas from the last glacial maximum vary only slightly from other published estimates, and we similarly find that these five basins remained enclosed during that time [*Mifflin and Wheat*, 1979; *Allison*, 1982; *Freidel*, 1993; *Reheis*, 1999]. Surveyed shore platforms are 2–25 m wide, roughly an order of magnitude smaller than theoretical maxima. This size may reflect limited time that the paleolakes occupied each topographic level. The small size would make these shore landforms highly susceptible to impact gardening on Mars, particularly on steep slopes, where cratering may have facilitated mass wasting. We find that preservation of shore landforms from the Noachian Period is highly unlikely, as most impact craters <4–8 km in diameter are missing from the geologic record. Early Hesperian surfaces are saturated with craters $<\sim$200 m in diameter, resulting in $\sim$20 m of impact gardening [*Hartmann et al.*, 2001], which would also eradicate features of the scale observed here.

[34] If the Martian highlands experienced a peak pluvial climate up to that of the Great Basin, which some recent work suggests [*Matsubara et al.*, 2011], then crater paleolakes may have been numerous, but they would not necessarily have been deep. Even at peak climatic conditions, the studied Great Basin paleolakes occupied only 19–37% of their respective watersheds, which would correspond to crater lakes on Mars that were 43–61% of the crater diameter. In many flat-floored, degraded craters, these lakes would have been shallow, and wave action may have never modified the crater walls. Depositional beach ridges, which may have formed on low-gradient crater floors, can be even more topographically subtle than erosional shore platforms and more susceptible to impact and aeolian modification. In that sense, neither slopes near the angle of repose nor low-gradient surfaces are ideal for the preservation of shore landforms.

[35] These results do not preclude the development and preservation of shore landforms on Mars, particularly in large basins. Identification of pluvial shore landforms may depend on a Late Hesperian or ideally later origin [e.g., *Boyce et al.*, 2005; *Mouginot et al.*, 2012], weak rocks, long fetch, and prolonged stability of the water level, which would allow larger forms to develop and resist degradation. However, a high latitude or other environmental conditions that would favor the development of an ice cover could offset the advantage of fetch in large basins [e.g., *Kraal et al.*, 2006]. Detection of well-preserved shore landforms of the scale observed here would require meter-scale imaging or topography, such as that currently available from HiRISE stereo DEMs. MOLA and even HRSC data [*Jaumann et al.*, 2007] have resolutions that are too coarse for this purpose. The studied shore landforms are often not equally well expressed around the entire perimeter of a basin, perhaps due to local differences in lithology, slope, and orientation to wind. For this reason, interpreting a correlation between shore landforms observed in plan view imaging alone can be challenging, and a lack of continuity in shore platform elevations around a basin does not exclude origin in a paleolake, as they may represent multiple water levels.

[36] **Acknowledgments.** A grant from the NASA Mars Fundamental Research Program (NNX07AQ71G; JRZ, Principal Investigator) funded the field investigation, and the Mars Data Analysis Program (NNX11AI92G, RPI, Principal Investigator) funded analysis of planetary data. We thank Tim Parker, Monica Pondrelli, and Nicolas Mangold for their constructive reviews. Much of this work was completed while RPI was a visiting scientist at NASA Goddard Space Flight Center, Greenbelt, Maryland.

References

Allison, I. S. (1966), *Fossil Lake, Oregon: Its Geology and Fossil Faunas*, *Oreg. State Monogr. Stud. Geol.*, vol. 9, 48 pp., Oreg. State Univ. Press, Corvallis.

Allison, I. S. (1979), *Pluvial Fort Rock Lake, Lake County, Oregon*, *Spec. Pap. Oreg. Dept. Geol. Miner. Ind.*, vol. 7, 72 pp., Dept. of Geol. and Miner. Ind., Portland, Oreg.

Allison, I. S. (1982), *Geology of Pluvial Lake Chewaucan, Lake County, Oregon*, *Oreg. State Monogr. Stud. Geol.*, vol. 11, 79 pp., Oreg. State Univ. Press, Corvallis.

Antevs, E. (1948), The Great Basin with emphasis of glacial and post-glacial times: Climatic changes and pre-white man, *Univ. Utah Bull.*, *38*, 167–191.

Benson, L. V. (1993), Factors affecting ^{14}C ages of lacustrine carbonates: Timing and duration of the last highstand lake in the Lahontan basin, *Quat. Res.*, *39*, 163–174.

Benson, L. V., D. R. Currey, R. I. Dorn, K. R. Lajoie, C. G. Oviatt, S. W. Robinson, G. I. Smith, S. Stine, and R. W. Thompson (1990), Chronology of expansion and contraction of four Great Basin lake systems during the past 35,000 years, *Palaeogeogr. Palaeoclimatol. Palaeoecol.*, *78*, 241–286, doi:10.1016/0031-0182(90)90217-U.

Boyce, J. M., P. Mouginis-Mark, and H. Garbeil (2005), Ancient oceans in the northern lowlands of Mars: Evidence from impact crater depth/diameter relationships, *J. Geophys. Res.*, *110*, E03008, doi:10.1029/2004JE002328.

Cabrol, N. A., and E. A. Grin (1999), Distribution, classification, and ages of Martian impact crater lakes, *Icarus*, *142*, 160–172, doi:10.1006/icar.1999.6191.

Cabrol, N. A., and E. A. Grin (2001), The evolution of lacustrine environments on early Mars: Is Mars only hydrologically dormant?, *Icarus*, *149*, 291–328, doi:10.1006/icar.2000.6530.

Carr, M. H., and J. W. Head III (2003), Oceans on Mars: An assessment of the observational evidence and possible fate, *J. Geophys. Res.*, *108*(E5), 5042, doi:10.1029/2002JE001963.

Cohen, A. S., M. R. Palacios-Fest, R. M. Negrini, P. E. Wigand, and D. B. Erbes (2000), A paleoclimate record for the past 250,000 years from Summer Lake, Oregon, U.S.A.: II. Sedimentology, paleontology, and geochemistry, *J. Paleolimnol.*, *24*, 151–182, doi:10.1023/A:1008165326401.

Davis, J. O. (1985), Correlation of late Quaternary tephra layers in a long pluvial sequence near Summer Lake, Oregon, *Quat. Res.*, *23*, 38–53, doi:10.1016/0033-5894(85)90070-5.

Fassett, C. I., and J. W. Head III (2008), Valley network-fed, open-basin lakes on Mars: Distribution and implications for Noachian surface and subsurface hydrology, *Icarus*, *198*, 37–56, doi:10.1016/j.icarus.2008.06.016.

Forbes, C. F. (1973), Pleistocene shoreline morphology of the Fort Rock basin, Oregon, PhD diss., Univ. of Oreg., Eugene.

Forsythe, R. D., and C. R. Blackwelder (1998), Closed drainage crater basins of the Martian highlands: Constraints on the early Martian hydrologic cycle, *J. Geophys. Res.*, *103*, 31,421–31,431, doi:10.1029/98JE01966.

Forsythe, R. D., and J. R. Zimbelman (1995), A case for ancient evaporite basins on Mars, *J. Geophys. Res.*, *100*, 5553–5563, doi:10.1029/95JE00325.

Freidel, D. E. (1993), Chronology and climatic controls of late Quaternary lake-level fluctuations in Chewaucan, Fort Rock, and Alkali basins, south-central Oregon, PhD diss., 244 pp., Univ. of Oreg., Eugene.

Freidel, D. E. (1994), Palaeolake shorelines and lake-level chronology of the Fort Rock basin, Oregon, in *Archaeological Researches in the Northern Great Basin: Fort Rock Archaeology Since Cressman*, *Anthropol. Pap.*, *50*, edited by C. M. Aikens and D. L. Jenkins, pp. 21–40, Dept. of Anthropol. and State Museum of Anthropol., Univ. of Oreg., Eugene.

Ghatan, G. J., and J. R. Zimbelman (2006), Paucity of candidate coastal constructional landforms along proposed shorelines on Mars: Implications for a northern lowlands-filling ocean, *Icarus*, *185*, 171–196, doi:10.1016/j.icarus.2006.06.007.

Golombek, M. P., et al. (2006), Erosion rates at the Mars Exploration Rover landing sites and long-term climate change on Mars, *J. Geophys. Res.*, *111*, E12S10, doi:10.1029/2006JE002754.

Grant, J. A., and S. A. Wilson (2011), Late alluvial fan formation in southern Margaritifer Terra, Mars, *Geophys. Res. Lett.*, *38*, L08201, doi:10.1029/2011GL046844.

Grant, J. A., et al. (2006), Crater gradation in Gusev crater and Meridiani Planum, Mars, *J. Geophys. Res.*, *111*, E02S08, doi:10.1029/2005JE002465.

Greeley, R., B. H. Foing, H. Y. McSween Jr., G. Neukum, P. Pinet, M. van Kan, S. C. Werner, D. A. Williams, and T. E. Zegers (2005), Fluid lava flows in Gusev crater, Mars, *J. Geophys. Res.*, *110*, E05008, doi:10.1029/2005JE002401.

Hartmann, W. K. (2005), Martian cratering 8. Isochron refinement and the history of Martian geologic activity, *Icarus*, *174*, 294–320, doi:10.1016/j.icarus.2004.11.023.

Hartmann, W. K., J. Anguita, M. A. de la Casa, D. C. Berman, and E. V. Ryan (2001), Martian cratering 7: The role of impact gardening, *Icarus*, *149*, 37–53, doi:10.1006/icar.2000.6532.

Hauber, E., K. Gwinner, M. Kleinhans, D. Reiss, G. Di Achille, G.-G. Ori, F. Scholten, L. Marinangeli, R. Jaumann, and G. Neukum (2009), Sedimentary deposits in Xanthe Terra: Implications for the ancient climate on Mars, *Planet. Space Sci.*, *57*, 944–957, doi:10.1016/j.pss.2008.06.009.

Head, J. W., H. Hiesinger, M. A. Ivanov, M. A. Kreslavsky, S. Pratt, and B. J. Thomson (1999), Possible ancient oceans on Mars: Evidence from Mars Orbiter Laser Altimeter data, *Science*, *286*, 2134–2137, doi:10.1126/science.286.5447.2134.

Holcomb, R. (1971), Terraced depressions in lunar maria, *J. Geophys. Res.*, *76*, 5703–5711, doi:10.1029/JB076i023p05703.

Hostetler, S., and L. V. Benson (1990), Paleoclimatic implications of the high stand of Lake Lahontan derived from models of evaporation and lake level, *Clim. Dyn.*, *4*, 207–217, doi:10.1007/BF00209522.

Huckleberry, G., C. Beck, G. T. Jones, A. Holmes, M. Cannon, S. Livingston, and J. M. Broughton (2001), Terminal Pleistocene/Early Holocene environmental change at the Sunshine Locality, North-Central Nevada, U.S.A, *Quat. Res.*, *55*, 303–312, doi:10.1006/qres.2001.2217.

Hynek, B. M., M. Beach, and M. R. T. Hoke (2010), Updated global map of Martian valley networks and implications for climate and hydrologic processes, *J. Geophys. Res.*, *115*, E09008, doi:10.1029/2009JE003548.

Irwin, R. P., III, and J. A. Grant (2012), Geologic map of MTM -15027, -20027, -25027 and -25032 quadrangles, Margaritifer Terra region of Mars, *U. S. Geol. Surv. Sci. Invest. Map*, in press.

Irwin, R. P., III, A. D. Howard, and T. A. Maxwell (2004), Geomorphology of Ma'adim Vallis, Mars, and associated paleolake basins, *J. Geophys. Res.*, *109*, E12009, doi:10.1029/2004JE002287.

Irwin, R. P., III, A. D. Howard, R. A. Craddock, and J. M. Moore (2005), An intense terminal epoch of widespread fluvial activity on early Mars: 2. Increased runoff and paleolake development, *J. Geophys. Res.*, *110*, E12S15, doi:10.1029/2005JE002460.

Irwin, R. P., III, R. A. Craddock, A. D. Howard, and H. L. Flemming (2011), Topographic influences on development of Martian valley networks, *J. Geophys. Res.*, *116*, E02005, doi:10.1029/2010JE003620.

Ivanov, M. A., and J. W. Head (2001), Chryse Planitia, Mars: Topographic configuration, outflow channel continuity and sequence, and tests for hypothesized ancient bodies of water using Mars Orbiter Laser Altimeter (MOLA) data, *J. Geophys. Res.*, *106*, 3275–3295, doi:10.1029/2000JE001257.

Jaumann, R., et al. (2007), The high-resolution stereo camera (HRSC) experiment on Mars Express: Instrument aspects and experiment conduct from interplanetary cruise through the nominal mission, *Planet. Space Sci.*, *55*, 928–952, doi:10.1016/j.pss.2006.12.003.

Kirk, R. L., et al. (2008), Ultrahigh resolution topographic mapping of Mars with MRO HiRISE stereo images: Meter-scale slopes of candidate Phoenix landing sites, *J. Geophys. Res.*, *113*, E00A24, doi:10.1029/2007JE003000.

Kraal, E. R., E. Asphaug, J. M. Moore, and R. D. Lorenz (2006), Quantitative geomorphic modeling of Martian bedrock shorelines, *J. Geophys. Res.*, *111*, E03001, doi:10.1029/2005JE002567.

Kuehn, S. C., and R. M. Negrini (2010), A 250 k.y. record of Cascade arc pyroclasic volcanism from late Pleistocene lacustrine sediments near Summer Lake, Oregon, USA, *Geosphere*, *6*, 397–429, doi:10.1130/GES00515.1.

Licciardi, J. M. (2001), Chronology of latest Pleistocene lake-level fluctuations in pluvial Lake Chewaucan basin, Oregon USA, *J. Quat. Sci.*, *16*, 545–553, doi:10.1002/jqs.619.

Lorenz, R. D., E. R. Kraal, E. E. Eddlemon, J. Cheney, and R. Greeley (2005), Sea-surface wave growth under extraterrestrial atmospheres: Preliminary wind tunnel experiments with application to Mars and Titan, *Icarus*, *175*, 556–560, doi:10.1016/j.icarus.2004.11.019.

Luo, W., and T. F. Stepinski (2009), Computer-generated global map of valley networks on Mars, *J. Geophys. Res.*, *114*, E11010, doi:10.1029/2009JE003357.

Malin, M. C., and K. S. Edgett (2001), Mars Global Surveyor Mars Orbiter Camera: Interplanetary cruise through primary mission, *J. Geophys. Res.*, *106*, 23,429–23,570, doi:10.1029/2000JE001455.

Masursky, H., J. M. Boyce, A. L. Dial, G. G. Schaber, and M. E. Strobell (1977), Classification and time of formation of Martian channels based on Viking data, *J. Geophys. Res.*, *82*, 4016–4038, doi:10.1029/JS082i028p04016.

Matsubara, Y., A. D. Howard, and S. A. Drummond (2011), Hydrology of early Mars: Lake basins, *J. Geophys. Res.*, *116*, E04001, doi:10.1029/2010JE003739.

McEwen, A. S., et al. (2007), Mars Reconnaissance Orbiter's High Resolution Imaging Science Experiment (HiRISE), *J. Geophys. Res.*, *112*, E05S02, doi:10.1029/2005JE002605.

Meinzer, O. E. (1922), map of the Pleistocene lakes of the Basin and Range province and its significance, *Geol. Soc. Am. Bull.*, *33*, 541–552.

Mifflin, M. D., and M. M. Wheat (1979), *Pluvial Lakes and Estimated Pluvial Climates of Nevada*, *Nev. Bur. of Mines Geol. Bull.*, vol. 94, Univ. of Nev., Reno.

Moore, J. M., and D. E. Wilhelms (2001), Hellas as a possible site of ancient ice-covered lakes on Mars, *Icarus*, *154*, 258–276, doi:10.1006/icar.2001.6736.

Mouginot, J., A. Pommerol, P. Beck, W. Kofman, and S. M. Clifford (2012), Dielectric map of the Martian northern hemisphere and the nature of plain filling materials, *Geophys. Res. Lett.*, *39*, L02202, doi:10.1029/2011GL050286.

Negrini, R. M., D. B. Erbes, K. Faber, A. M. Herrera, A. P. Roberts, A. S. Cohen, P. E. Wigand, and F. F. Foit (2000), A paleoclimate record for the past 250,000 years from Summer Lake, Oregon, USA: I. chronology and magnetic proxies for lake level, *J. Paleolimnol.*, *24*, 125–149, doi:10.1023/A:1008144025492.

Nordstrom, K. F., and N. L. Jackson (2012), Physical processes and landforms on beaches in short fetch environments in estuaries, small lakes and reservoirs: A review, *Earth Sci. Rev.*, *111*, 232–247, doi:10.1016/j.earscirev.2011.12.004.

O'Connor, J. E. (1993), Hydrology, hydraulics, and geomorphology of the Bonneville Flood, *Spec. Pap. Geol. Soc. Am.*, *274*, 83 pp.

Ori, G. G., L. Marinangeli, and A. Baliva (2000), Terraces and Gilbert-type deltas in crater lakes in Ismenius Lacus and Memnonia (Mars), *J. Geophys. Res.*, *105*, 17,629–17,641, doi:10.1029/1999JE001219.

Oviatt, C. G. (1997), Lake Bonneville fluctuations and global climate change, *Geology*, *25*, 155–158, doi:10.1130/0091-7613(1997)025<0155:LBFAGC>2.3.CO;2.

Parker, T. J. (1985), Geomorphology and geology of the southwestern Margaritifer Sinus-Northern Argyre region of Mars, Master's thesis, Calif. State Univ., Los Angeles.

Parker, T. J. (1994), Martian paleolakes and oceans, PhD thesis, 200 pp., Univ. of South. Calif., Los Angeles.

Parker, T. J., and D. R. Currey (2001), Extraterrestrial coastal geomorphology, *Geomorphology*, *37*, 303–328, doi:10.1016/S0169-555X(00)00089-1.

Parker, T. J., R. S. Saunders, and D. M. Schneeberger (1989), Transitional morphology in West Deuteronilus Mensae, Mars: Implications for modification of the lowland/upland boundary, *Icarus*, *82*, 111–145, doi:10.1016/0019-1035(89)90027-4.

Parker, T. J., D. S. Gorsline, R. S. Saunders, D. C. Pieri, and D. M. Schneeberger (1993), Coastal geomorphology of the Martian northern plains, *J. Geophys. Res.*, *98*, 11,061–11,078, doi:10.1029/93JE00618.

Parker, T. J., J. A. Grant, and B. J. Franklin (2010), The northern plains: A Martian oceanic basin?, in *Lakes on Mars*, edited by N. A. Cabrol and

E. A. Grin, pp. 249–273, Elsevier, New York, doi:10.1016/B978-0-444-52854-4.00009-X.

Pieri, D. C. (1980), Geomorphology of Martian valleys, in *Advances in Planetary Geology*, *NASA Tech. Memo.*, *TM-81979*, 160 pp.

Reheis, M. (1999), *Extent of Pleistocene Lakes in the Western Great Basin*, *U. S. Geol. Surv. Misc. Field Stud. Map*, *MF-2323*.

Reichert, K. L., J. M. Licciardi, and D. S. Kaufman (2011), Amino acid racemization in lacustrine ostracodes, part II: Paleothermometry in Pleistocene sediments at Summer Lake, Oregon, *Quat. Geochronol.*, *6*, 174–185, doi:10.1016/j.quageo.2010.11.007.

Russell, I. C. (1884), A geological reconnaissance in southern Oregon, *U. S. Geol. Surv. Annu. Rep.*, *4*, 431–464.

Russell, I. C. (1905), Preliminary report on the geology and water resources of central Oregon, *U. S. Geol. Surv. Bull.*, *252*, 138 pp.

Smith, D. E., et al. (2001), Mars Orbiter Laser Altimeter: Experiment summary after the first year of global mapping of Mars, *J. Geophys. Res.*, *106*, 23,689–23,722, doi:10.1029/2000JE001364.

Snyder, C. T., G. Hardman, and F. F. Zdenek (1964), Pleistocene lakes in the Great Basin, *U. S. Geol. Surv. Misc. Geol. Invest. Map*, *I-416*.

Tanaka, K. L., J. A. Skinner Jr., T. M. Hare, T. Joyal, and A. Wenker (2003), Resurfacing history of the northern plains of Mars based on geologic mapping of Mars Global Surveyor data, *J. Geophys. Res.*, *108*(E4), 8043, doi:10.1029/2002JE001908.

Tazieff, H. (1994), Permanent lava lakes: Observed facts and induced mechanisms, *J. Volcanol. Geotherm. Res.*, *63*, 3–11, doi:10.1016/0377-0273(94)90015-9.

Thelin, G. P., and R. J. Pike (1991), Landforms of the conterminous United States— A digital shaded-relief portrayal, *U. S. Geol. Surv. Misc. Geol. Invest. Map*, *I-2206*.

Thompson, R. S., P. J. Bartlein, C. Whitlock, S. P. Harrison, and W. G. Spaulding (1993), *Climatic Changes in the Western United States Since 18,000 Years B.P*, Univ. of Minn. Press, Minneapolis.

Trenhaile, A. S. (2001), Modelling the Quaternary evolution of shore platforms and erosional continental shelves, *Earth Surf. Processes Landforms*, *26*, 1103–1128, doi:10.1002/esp.255.

Walker, G. W., and N. S. MacLeod (1991), Geologic map of Oregon, 2 plates, scale 1:500,000, U.S. Geol. Survey, Denver, Colo.

Wilson, S. A., J. M. Moore, A. D. Howard, and D. E. Wilhelms (2010), Evidence for ancient lakes in the Hellas region, in *Lakes on Mars*, edited by N. Cabrol and E. Grin, pp. 195–222, Elsevier, Oxford, U. K., doi:10.1016/B978-0-444-52854-4.00007-6.

Zic, M., R. M. Negrini, and P. E. Wigand (2002), Evidence of synchronous climate change across the Northern Hemisphere between the North Atlantic and the northwestern Great Basin, United States, *Geology*, *30*, 635–638, doi:10.1130/0091-7613(2002)030<0635:EOSCCA>2.0.CO;2.

Zimbelman, J. R., and R. P. Irwin III (2008), Field investigations of pluvial features in the western United States as analogs to features on Mars, *Lunar Planet. Sci.*, *XXXIX*, Abstract 1148.

Zimbelman, J. R., and A. K. Johnston (2001), Improved topography of the Carrizozo lava flow: Implications for emaplacement conditions, in *Volcanology in New Mexico*, *Bull. 18*, edited by L. S. Crumpler and S. G. Lucas, pp. 131–136, N. M. Museum of Nat. Hist. and Sci., Albuquerque, N. M.

Zimbelman, J. R., W. B. Garry, and R. P. Irwin III (2009), Precision topography of pluvial features in western Nevada as analogs for possible pluvial landforms on Mars, *Lunar Planet. Sci.*, *XL*, Abstract 1370.